BSTR, 2023, Vol 11, No 1, 23-32
https://doi.org/10.54987/bstr.v11i1.833

HIBISCUS PUBLISHER

BIOREMEDIATION SCIENCE AND TECHNOLOGY RESEARCH

Website: http://journal.hibiscuspublisher.com/index.php/BSTR/index

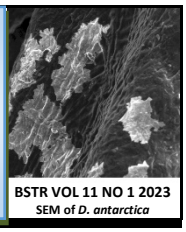

Mercury Sorption onto Rice Husk Ash: An Isothermal Remodelling

Bilal Ibrahim Dan-Iya[1], Faggo Abdullahi Adamu[1,2], Muhammed Abdullahi Ubana[1,3], Ismail Haruna[1,2], Aisha Grema[1] and Mohd Yunus Shukor[1]*

[1]Department of Biochemistry, Faculty of Biotechnology and Biomolecular Sciences, Universiti Putra Malaysia, 43400 UPM Serdang, Selangor, Malaysia.
[2]Department of Microbiology, Faculty of Science, Bauchi State University Gadau, Bauchi, PMB 065, Nigeria.
[3]Department of Biochemistry and Molecular Biology, Faculty of Natural and Applied Sciences, Nasarawa State University, P.M.B 1022, Keffi, Nigeria.

*Corresponding author:
Mohd Yunus Shukor,
Department of Biochemistry,
Faculty of Biotechnology and Biomolecular Sciences,
Universiti Putra Malaysia,
43400 UPM Serdang,
Selangor,
Malaysia.
Email: mohdyunus@upm.edu.my

HISTORY

Received: 3rd March 2023
Received in revised form: 25th June 2023
Accepted: 29th July 2023

KEYWORDS

Mercury
Rice Husk
Remodelling
Isotherms
Freundlich

ABSTRACT

The rice milling process produces rice husk as a by-product. It is one of the most important agricultural leftovers in terms of volume. The data of the sorption isotherm of Hg (II) (CV) sorption onto rice husk ash, which was plotted using linearized plots of isothermal models were reanalyzed using isothermal models using nonlinear regression. As the datapoints were small, nineteen isotherm models with parameters of only up to three were utilized to prevent overfitting. The models were Henry, Langmuir, Freundlich, Temkin, Dubinin-Radushkevich, Jovanovic, Redlich-Peterson, Sips, Toth, Hill, Khan, BET, Vieth-Sladek, Radke-Prausnitz, Brouers–Sotolongo, Fritz-Schlunder III, Unilan, Fowler-Guggenheim and Moreau. Statistical analysis based on error function analyses such as root-mean-square error (RMSE), adjusted coefficient of determination (adjR^2), accuracy factor (AF), bias factor (BF), Bayesian Information Criterion (BIC), corrected AICc (Akaike Information Criterion), and Hannan-Quinn Criterion (HQC) showed that Freundlich model was the best model. The value of the maximum monolayer adsorption capacity for Hg binding to rice husk ash according to the Langmuir's parameter q_{mL} was 3.998 mg g-1 (95% Confidence interval from 2.473 to 5.523), while b_L (L mg^{-1}), the Langmuir model constants was 0.067 L mg-1 (95% C.I. from 0.001 to 0.134). The Freundlich model is unable to forecast the maximal adsorption capacity. The Halsey rearrangement of the Freundlich equation gave the estimated maximum absorption of 3.39 mg g^{-1}, which is very close to the experimental value. The nonlinear regression method provides parameter values within the 95% confidence interval, facilitating improved comparability with prior research.

INTRODUCTION

Since many decades ago, one of the most significant concerns has been the poisoning of water systems across the world with heavy metals. It is well acknowledged that some metals pose a threat to the health of a variety of different forms of life. The Metals Cr, Cu, Pb, Zn, and Hg stand out as some of the most dangerous pollutants on the list of pollutants that are included in the water framework directive (Directive 2000/60/EC) [1]. Over the course of the past several years, various countries have introduced brand new regulations, tightened existing ones, and increased their level of enforcement regarding wastewater discharges. Organic mercury is a third form of mercury that exists alongside inorganic mercury and elemental mercury that is metallic (methylmercury). These sorts have varying degrees of impact on human organs such the gastrointestinal tract, the central nervous system, the immune system, the skin, the eyes, and the respiratory system. The amount of mercury released into the environment as a result of human activities, such as the generation of electricity through the processing of industrial waste, the burning of coal, the incineration of waste at homes, and the mining of mercury (along with gold and other metals), has significantly increased [2–8].

Methylmercury is a type of mercury that bacteria may convert into under using their unique enzymes. It builds up in marine species and flows biomagnetically up the food chain, such that predatory fish like sharks and rays have higher concentrations of it than fish with a lower body size. Inhalation of elemental mercury vapors found in industrial environments is one way that mercury can enter the body. Another way is through

the ingestion of fish and shellfish that have been polluted. Mercury is not removed from the body by cooking it [2,3,5,9–12].

Treatment centers are currently using some of the novel and much improved approaches that have been developed in response to this issue. Several different treatment processes have been proposed as possible solutions for eliminating heavy metals from water sources in the existing literature. Among the techniques that fit this description are coagulation, chemical precipitation, evaporation, electrolysis, adsorption, and reverse osmosis. On the other hand, these conventional forms of technology may be insufficient, too costly, or even cause new problems. It's effective and cost-efficient , and it's easy to execute. Therefore, adsorption is likely to be the most popular approach. Future progress may be hampered, however, by the cost of the adsorbent and the energy needed to keep it refilled.

Biosorption, a risk-free and cost-effective method for cleaning polluted water, is widely adopted for this purpose. Biosorbents can be made from either biomass or natural substrates. There has been a lot of research on the topic of mercury biosorption published in recent years [13–23]. The quality of this study is exceptional, and it was not conducted at an unreasonably high expense. Adsorbents with cheap costs include those that are plentiful in nature or created as a byproduct of industrial processes, and those that may be acquired in vast numbers with little to no additional expense. There has been a rise in interest in employing inexpensive materials for absorbent applications, which is in line with the growing importance of the issue of recycling garbage and similar resources.

This is becoming increasingly important in many fields, including adsorptive materials where there is a rising need and desire for more cost-effective solutions. Because rice husk can be burnt to generate steam, many different types of enterprises may save money by cutting back on their usage of both energy and raw materials. Ash from boilers and furnaces that burn rice husks is known as rice husk ash. This ash is collected in a dust collector located upstream from the stacks. Ash remaining after burning rice husk is sometimes called "rice husk ash."Adsorbents like rice husk and ash are cheap and readily available in Malaysia [24–28], thus researchers have started using them in their work. The studies employed the utilization of these adsorbents.

The accurate assignment of the kinetics and isotherms of biosorption is an absolutely necessary step in gaining an understanding of the biosorption process in these particular species. In many cases, the published research will provide a linearized form of an obviously nonlinear curve that these data produce. The error structure of the data is affected when nonlinear data is linearized, which makes it more difficult to assess uncertainty, which is often expressed as a confidence range of 95 percent. The purpose of this study is to rework a previously published study on the sorption of zinc on rice husk ash [29], which utilize linear regression to obtain best fitting models.

METHOD

Data acquisition and fitting

Figure 2 data from a previously published study [29] was digitized using the freeware Webplotdigitizer 2.5 [30]. After that, the data were nonlinearly regressed using the curve-fitting program Curve-Expert Professional (Version 2.6.5, Copyrights 2011-2017, Daniel G. Hyams). Digitization using this program has been praised for its dependability [31,32].

Isotherms

As the value of the datapoints is very small, only models having parameters of up to three were considered to prevent overfitting. Nineteen models were tested.

Table 1. Mathematical models that were used in modelling data [33,34].

Isotherm	*p*	Formula	Ref.
Henry's law	1	$q_e = HC_e$	[35]
Langmuir	2	$q_e = \frac{q_{mL} b_L C_e}{1 + b_L C_e}$	[33]
Jovanovic	2	$q_e = q_{mJ}(1 - e^{-K_J C_e})$	[36]
Freundlich	2	$q_e = K_F C_e^{\frac{1}{n_F}}$	[37]
Dubinin-Radushkevich	2	$q_e = q_{mDR} exp\left\{-K_{DR}\left[RTln\left(1+\frac{1}{C_e}\right)\right]^2\right\}$	[38,39]
Temkin	3	$q_e = \frac{RT}{b_T}\{ln(a_T C_e)\}$	[40,41]
Redlich-Peterson	3	$q_e = \frac{K_{RP1} C_e}{1 + K_{RP2} C_e^{\beta_{RP}}}$	[42]
Sips	3	$q_e = \frac{K_s q_{mS} C_e^{\frac{1}{n_S}}}{1 + K_s C_e^{\frac{1}{n_S}}}$	[43]
Toth	3	$q_e = \frac{q_{mT} C_e}{\left(K_T + C_e^{n_T}\right)^{n_T}}$	[44]
Hill	3	$q_e = \frac{q_{mH} C_e^{n_H}}{K_H + C_e^{n_H}}$	[45]
Khan	3	$q_e = \frac{q_{mK} b_K C_e}{(1 + b_K C_e)^{a_K}}$	[46]
BET	3	$q_e = \frac{q_{mBET} \alpha_{BET} C_e}{(1 - \beta_{BET} C_e)(1 - \beta_{BET} C_e + \alpha_{BET} C_e)}$	[47]
Vieth-Sladek	3	$q_e = \frac{q_{mVS} b_{VS} C_e}{(1 + b_{VS} C_e)^{n_{VS}}}$	[48]
Radke-Prausnitz	3	$q_e = \frac{q_{mRP} K_{RP} C_e}{(1 + K_{RP} C_e)^{n_{RP}}}$	[49]
Brouers–Sotolongo	3	$q_e = q_{mBS}\left(1 - \exp\left(-K_{BS} C_e^{\frac{1}{n_{BS}}}\right)\right)$	[50]
Fritz-Schlunder-III	3	$q_e = \frac{q_{mFS} K_{FS} C_e}{1 + K_{FS} C_e^{n_{FS}}}$	[51]
Fowler-Guggenheim*	3	$q_e = q_{mFG} \frac{K_L C_e e^{\frac{\alpha q_e}{q_{mFG}}}}{1 + K_L C_e e^{\frac{\alpha q_e}{q_{mFG}}}}$	[52]
Moreau	3	$q_e = q_{mM} \frac{bC_e + lb^2 C_e^{\,2}}{1 + 2bC_e + lb^2 C_e^{\,2}}$	[53]
Unilan	3	$q_e = \frac{q_{mU}}{2b_U} ln\left(\frac{a_U + C_e e^{b_U}}{a_U + C_e e^{-b_U}}\right)$	

Note *Implicit equation or function.

Statistical analysis

A set of statistical discriminatory tests such as corrected AICc (Akaike Information Criterion), Bayesian Information Criterion (BIC), Hannan and Quinn's Criterion (HQ), Root-Mean-Square Error (RMSE), bias factor (BF), accuracy factor (AF) and adjusted coefficient of determination (R^2) were used in this study. The RMSE was computed using Equation 1, and it stands to reason that the fewer parameters utilized, the smaller the RMSE will be. n is for the total number of observations made in the experiment, Obi and Pdi stand for the total number of observations made in the experiment and projections, and p stands for the total number of parameters [54] .

$$RMSE = \sqrt{\frac{\sum_{i=1}^{n}(Pd_i - Ob_i)^2}{n-p}} \qquad \text{(Eqn. 1)}$$

The modified R^2 is used to get around the fact that R^2, also known as the coefficient of determination, does not take into account the number of parameters in a model. In the equation, S^2_y represents the total variance of the y-variable.(**Equations 2** and **3**), while RMS is the Residual Mean Square.

$$Bias\ factor = 10\left(\sum_{i=1}^{n} log\frac{(Pd_i/Ob_i)}{n}\right) \quad \text{(Eqn. 2)}$$

$$Accuracy\ factor = 10\left(\sum_{i=1}^{n} log\frac{|(Pd_i/Ob_i)|}{n}\right) \quad \text{(Eqn. 3)}$$

In **Equation 4**, the AICc is calculated as, where p is the total number of parameters and n is the total number of observations. When dealing with data that has many parameters but few values, the corrected Akaike information criterion (AICc) is applied. [55]. A model with a lower AICc score is considered more likely to be right [55]. It finds a favorable medium between a model's simplicity and its accuracy [56].

$$AICc = 2p + n\ln\left(\frac{RSS}{n}\right) + \frac{2(p+1)+2(p+2)}{n-p-2} \quad \text{(Eqn. 4)}$$

The Bayesian Information Criterion (BIC) is another information-theory-based statistical tool (BIC) (Equation 5). The number of parameters receives a harsher penalty from this error function than it does from the AIC [30].

$$BIC = n\ln\left(\frac{RSS}{n}\right) + k\ln(n) \quad \text{(Eqn. 5)}$$

Another method for analyzing error functions that is grounded in information theory is called the Hannan-Quinn information criterion (HQC) (**Equation 6**). Because of the *ln ln* n element in the calculation, the HQC is more consistent than the AIC [55].

$$HQC = nIn\left(\frac{RSS}{n}\right) + 2k\ln(\ln n) \quad \text{(Eqn. 6)}$$

Two more error function analyses that were derived from Ross's work are referred to as the Accuracy Factor (AF) and the Bias Factor (BF) [55]. These error functions do statistical evaluations of models to see how well they fit data, but they do not punish models based on the number of parameters (**Equations 7** and **8**).

$$Adjusted\ (R^2) = 1 - \frac{RMS}{S_Y^2} \quad \text{(Eqn. 4)}$$

$$Adjusted\ (R^2) = 1 - \frac{(1-R^2)(n-1)}{(n-p-1)} \quad \text{(Eqn. 5)}$$

RESULTS AND DISCUSSION

The equilibrium data from [57] was analyzed making use of the models—Henry, Langmuir, Freundlich, Redlich-Petersen, Sips, BET, Toth, Hill, Khan, Vieth-Sladek, Radke-Prausnitz, Unilan, Fritz-Schlunder III, Fritz-Schlunder IV, and Fritz-Schlunder V, were employed in determining the best fit by making use of non-linear regression. Henry, Langmuir, Hill, Vieth-Sladek, Unilan, Sips, and BET do not match well with the data, however Freundlich, Redlich-Petersen, Toth, Khan, Radke-Prausnitz, Fritz-Schlunder III, Fritz-Schlunder IV, and Fritz-Schlunder V did fit well with the data. Henry, Langmuir, Hill, Vieth-Sladek, Unilan, Sips (**Figs. 1 – 19**).

We discovered that the Freundlich isotherm model had the best combination of low values for AICc, BIC, HQC, and RMSE, as well as values of AF, BF, and adjR^2 that were closest to unity. This made the Freundlich isotherm model the model with the best overall fit. As a result of this, it was the most accurate model for describing isotherms. Following this is the Langmuir model, which is followed by the Jovanovic model, which is followed by the Fritz-Schlunder III model, and then lastly the Toth model (**Table 2**). It discusses and supports the greater accuracy of employing nonlinear regression as opposed to the linear regression employed in the original study, which suggests the 2-parameter Jovanovic isotherm as the best model because enough models fitted well with the burned rice husk data.

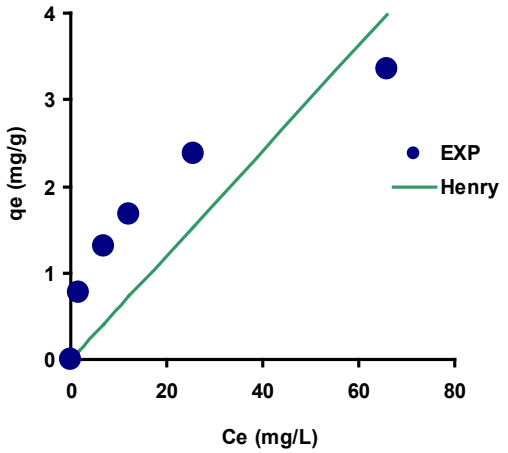

Fig. 1. Adsorption isotherm of Hg (II) onto rice husk ash as modelled using the Henry model.

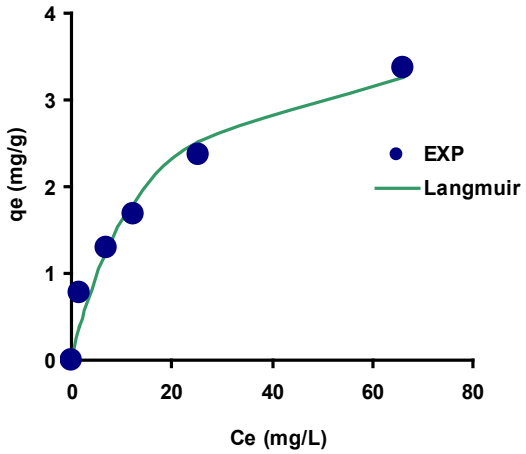

Fig. 2. Adsorption isotherm of Hg (II) onto rice husk ash as modelled using the Langmuir isotherm model.

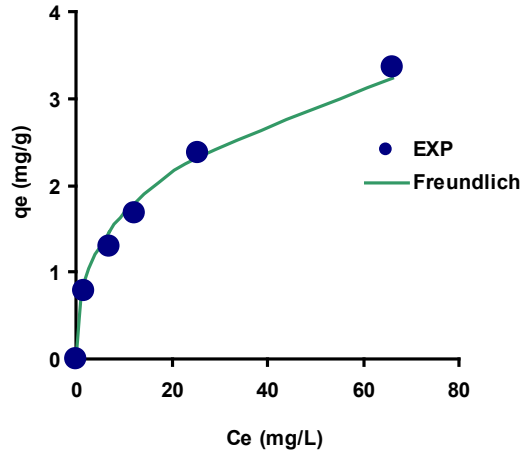

Fig. 3. Adsorption isotherm of Hg (II) onto rice husk ash as modelled using the Freundlich isotherm model.

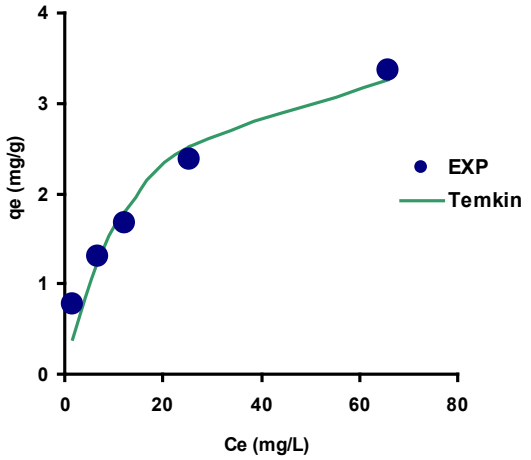

Fig. 4. Adsorption isotherm of Hg (II) onto rice husk ash as modelled using the Temkin isotherm model.

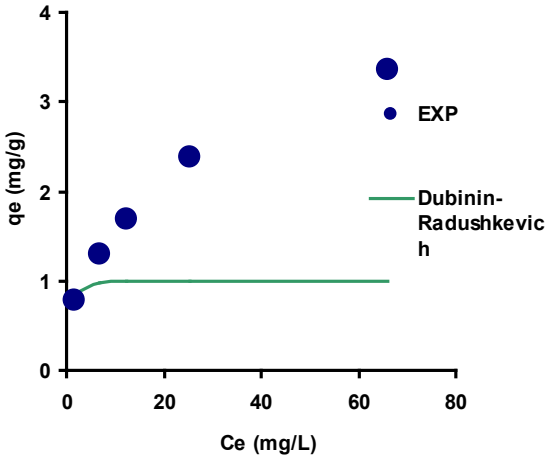

Fig. 5. Adsorption isotherm of Hg (II) onto rice husk ash as modelled using the Dubinin-Radushkevich isotherm model.

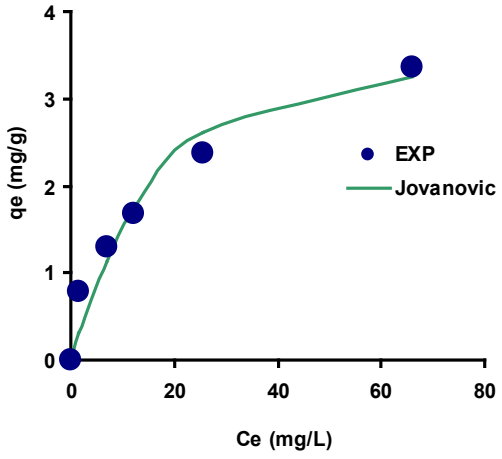

Fig. 6. Adsorption isotherm of Hg (II) onto rice husk ash as modelled using the Jovanovic isotherm model.

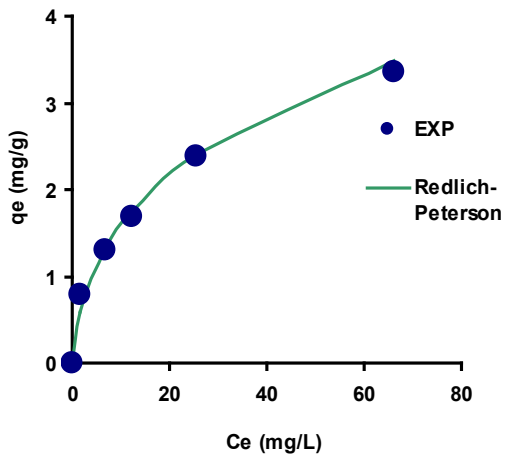

Fig. 7. Adsorption isotherm of Hg (II) onto rice husk ash as modelled using the Redlich-Peterson isotherm model.

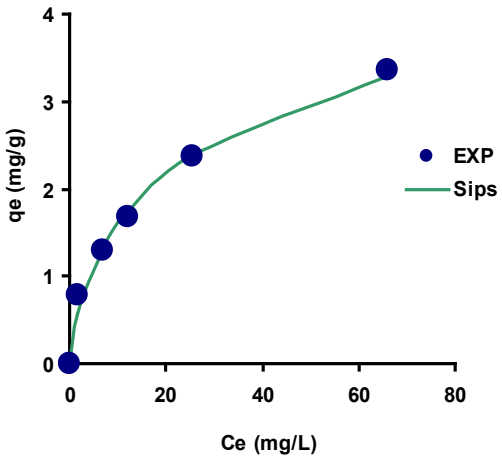

Fig. 8. Adsorption isotherm of Hg (II) onto rice husk ash as modelled using the Sips isotherm model.

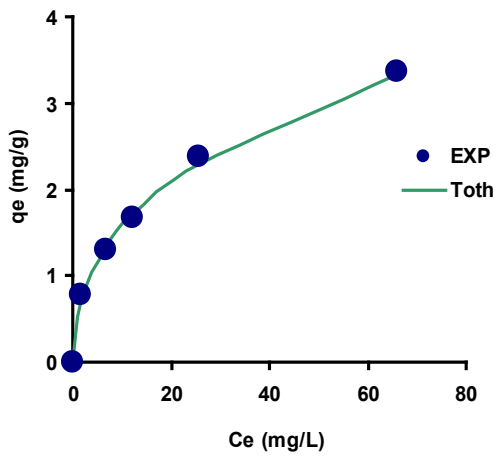

Fig. 9. Adsorption isotherm of Hg (II) onto rice husk ash as modelled using the Toth isotherm model.

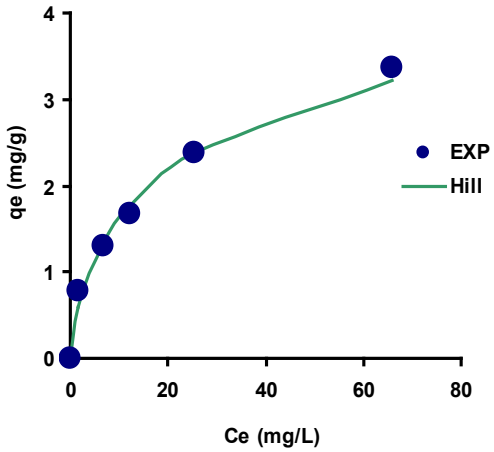

Fig. 10. Adsorption isotherm of Hg (II) onto rice husk ash as modelled using the Hill isotherm model.

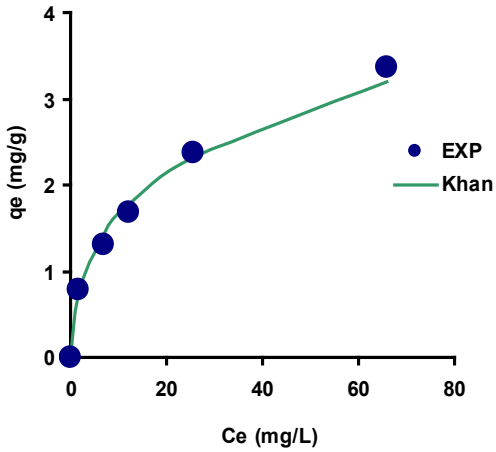

Fig. 11. Adsorption isotherm of Hg (II) onto rice husk ash as modelled using the Khan isotherm model.

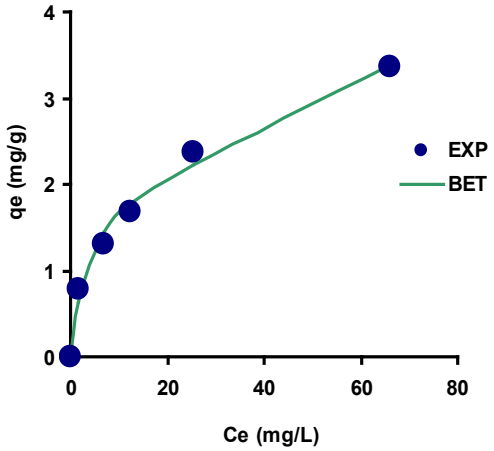

Fig. 12. Adsorption isotherm of Hg (II) onto rice husk ash as modelled using the BET isotherm model.

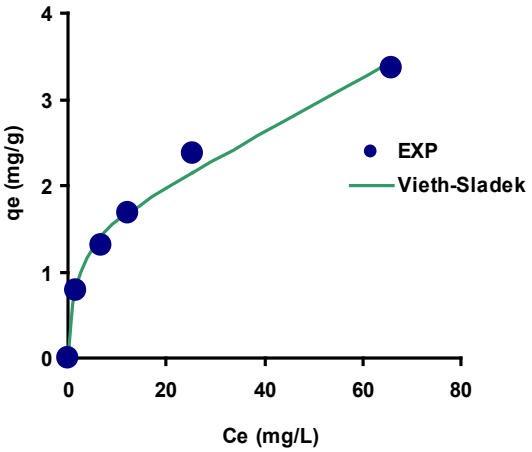

Fig. 13. Adsorption isotherm of Hg (II) onto rice husk ash as modelled using the Vieth-Sladek isotherm model.

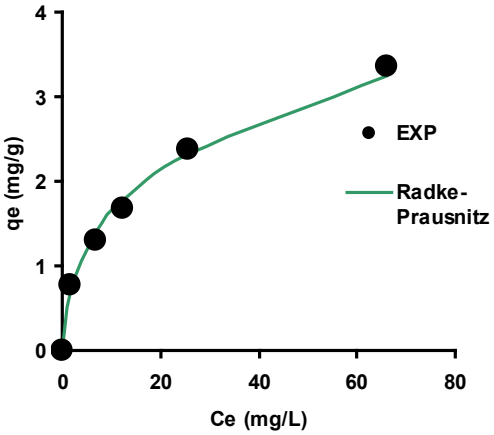

Fig. 14. Adsorption isotherm of Hg (II) onto rice husk ash as modelled using the Radke-Prausnitz isotherm model.

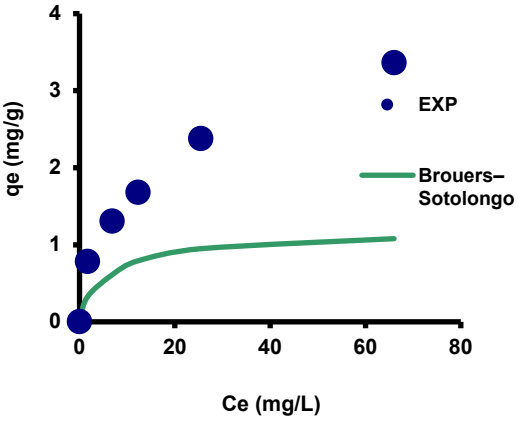

Fig. 15. Adsorption isotherm of Hg (II) onto rice husk ash as modelled using the Brouers-Sotolongo isotherm model.

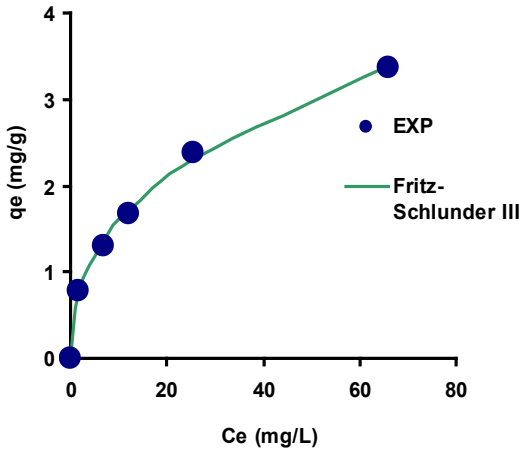

Fig. 16. Adsorption isotherm of Hg (II) onto rice husk ash as modelled using the Fritz-Schlunder III isotherm model.

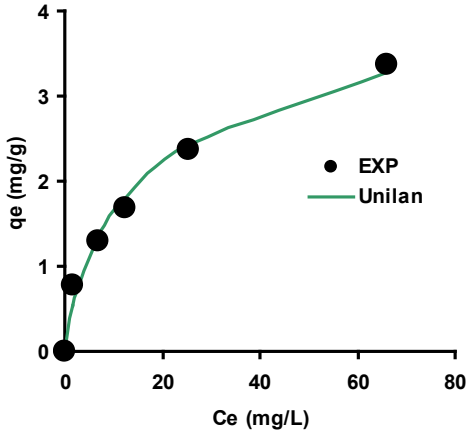

Fig. 17. Adsorption isotherm of Hg (II) onto rice husk ash as modelled using the Unilan isotherm model.

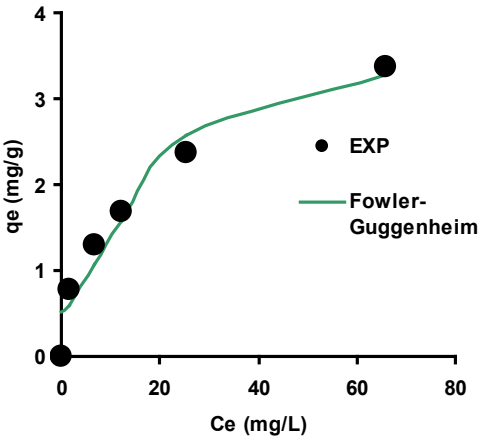

Fig. 18. Adsorption isotherm of Hg (II) onto rice husk ash as modelled using the Fowler Guggenheim isotherm model.

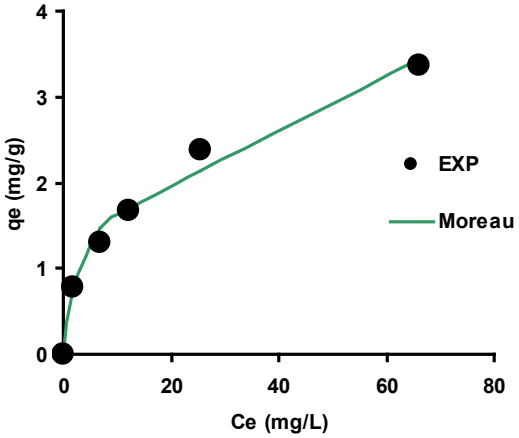

Fig. 19. Adsorption isotherm of Hg (II) onto rice husk ash as modelled using the Moreau isotherm model.

Table 2. Error function analysis for the fitting of the isotherm of Hg (II) onto rice husk ash.

Model	*p*	RMSE	adR^2	AICc	BIC	HQC	BF	AF
Henry	1	0.80	0.64	6.30	6.30	-1.91	0.49	2.17
Langmuir	2	0.22	0.96	1.48	1.48	-16.94	0.90	1.16
Freundlich	2	0.13	0.98	-5.25	-5.25	-23.66	1.04	1.06
Temkin	2	0.22	0.96	1.48	1.48	-16.94	0.90	1.16
Dubinin	2	1.42	-15.89	23.77	23.77	5.35	0.63	1.64
Jovano	2	0.28	0.93	4.36	4.36	-14.05	0.85	1.22
Red-Pet	3	0.14	0.98	26.08	26.08	-22.54	0.97	1.07
Sips	3	0.14	0.98	26.21	26.21	-22.42	0.95	1.07
Toth	3	0.08	0.99	19.94	19.94	-28.68	0.98	1.04
Hill	3	0.14	0.98	26.30	26.30	-22.32	0.96	1.07
Khan	3	0.14	0.98	26.13	26.13	-22.49	1.00	1.05
BET	3	0.15	0.98	27.32	27.32	-21.31	0.98	1.07
Vieth-S	3	0.15	0.98	27.20	27.20	-21.42	1.01	1.04
Radke-Prausnitz	3	0.13	0.98	25.06	25.06	-23.57	0.99	1.06
Brouers-Sotolongo	3	1.71	-25.60	56.25	56.25	7.63	0.48	2.10
Fritz-Schlunder III	3	0.06	1.00	15.71	15.71	-32.92	1.00	1.02
Unilin	3	0.17	0.97	28.56	28.56	-20.06	0.96	1.09
Fowler-Guggenheim	3	0.37	0.83	38.03	38.03	-10.59	0.924	0.92
Moreau	3	0.18	0.97	29.00	29.00	-19.62	1.001	1.00

Note:
RMSE Root mean Square Error
adR^2 Adjusted Coefficient of determination
p no of parameters
AF Accuracy factor
BF Bias factor
BIC Bayesian Information Criterion
AICc Adjusted Akaike Information Criterion
HQC Hannan–Quinn information criterion

Langmuir isotherm

There are many different models of isotherms, the most well-known of which is the Langmuir isotherm, which being entirely mechanical. The model assumed that adsorbate would be uniformly adsorbed onto the adsorbent. The isotherm works under the assumption that the structure of the adsorbent is consistent throughout, as well as that the energy of each adsorption site is the same [58]. Due to the ex-ponential decrease in intermolecular interactions with increasing distance, this isotherm model predicts the appearance of monolayer coverage of the adsorbent at the adsorbent's outer surface. This is the result of the adsorbent's growing distance from the solute. This model additionally streamlines the linear connection and makes the prediction of a constant capacity for adsorption by a monolayer.

On the basis of this, it is believed that Henry's model will be accurate for solutions ranging from those that are extremely diluted to those that are exceedingly concentrated [59]. In sorption research, including Zn sorption research, two of the models that are employed most frequently are the Langmuir model and the Freundlich model. The non-linear regression technique predicted a maximum adsorption parameter and model constant that were almost equal to those found in the original investigation; nevertheless, it was unable to create a confidence range for the projected values that contained 95% of the true value.

Freundlich isotherm

A well-known example of an empirical model for adsorption and desorption is the Freundlich equation, which was initially devised for the gas phase. In a Freun-dlich adsorption isotherm, the adsorbate forms a monomolecular layer on the surface of the adsorbent. The Freundlich equation offers some relevant empirical data on particle sorption; but, after a certain concentration, it changes its behavior and becomes nonlinear; as a result, its applicability is restricted [60–62]. In contrast to the Langmuir isotherm, the Freundlich model can be extended in order to take into account adsorption that occurs across many layers.

The results of this isotherm model suggest that the heat of adsorption and the affinities of molecules that have been adsorbed might be unevenly distributed across a surface that is composed of different types of matter. The exponential distribution of active sites, in addition to the energy and surface heterogeneity, are both defined by the statement that makes up the Freundlich isotherm model. The Freundlich isotherm model was initially used in the attempt to characterize the steps of adsorption of adsorbate onto the adsorbent charcoal. This was done in an attempt to determine how well the process worked. There was an alteration in the mass ratio of the adsorbate that was coupled to the adsorbent whenever there was an increase in the concentration of the solution.

This leads one to the conclusion that the total amount of adsorption which takes place at each location is equal to the quantity that is adsorbed. After the most stable binding sites are fully occupied, the amount of energy that is needed for adsorption begins to decrease at a pace that is exponential in nature [59,63,64]. Additionally, the Freundlich model was the most accurate representation of lead(II) sorption by a modified Jordanian zeolite [65], *Chlorococcum aquaticum* biomass [66], by a Guar gum/bentonite bionanocomposite [67], the sorption of other metal and radionuclides [68–73] and nanoparticle adsorbents of cellulose origin [74].

The Freundlich model, due to the empirical character of its data, is unable to make accurate predictions regarding the maximal adsorption capacity at which K_F ((mg g^{-1}.L mg^{-1})$^{1/nF}$) is the Freundlich isotherm constant, and n_F is the Freundlich exponent. A small $1/n_F$ value indicates a heterogenous system [60,75]. Due to the inability of the Freundlich equation to predict maximal adsorption, the Halsey restructuring of the Freundlich equation was developed [76] (**Equation 6**) gave the estimated maximum absorption of 3.39 mg g^{-1}, which is very close to the experimental value.

$$K_F = \frac{q_{mF}}{C_e^{\frac{1}{n_F}}} \qquad \text{(Eqn. 6)}$$

Temkin isotherm

In the Temkin isothermal model, which was developed by Temkin and Pyzner, adsorption is described as a constant function of temperature until it reaches its maximum binding energy [40]. Because of indirect adsorbate-adsorbate interactions over the surface of the heterogeneous material, the amount of surface coverage causes a drop in the heat of adsorption that is linearly proportional to the amount of surface coverage. The Temkin isotherm is constructed with the adsorption isotherm developed by Langmuir as its foundation. The positive heat produced by adsorption demonstrates that adsorption is an exothermic process ($b_T > 0$). The widely used Temkin model that is shown below is faulty as a result of a disparity in the dimensions between the left side of the equation and the right side of the equation;

$$q_e = \frac{RT}{b_T}\{ln(a_T C_e)\} \qquad \text{(Eqn. 33)}$$

The accurate application of the Temkin model, which Chu has just brought to light and improved, is summarized in the following [41];

$$\frac{q_e}{q_{mT}} = \frac{RT}{b_T}\left(ln(K_T C_e)\right) \qquad \text{(Eqn. 34)}$$

Where,

In this equation, K_T is the adsorption equilibrium constant of the solute on the solid surface expressed as L mg^{-1}, solute equilibrium concentration (C_e) is mg L^{-1}, q_e and q_m are the equilibrium and saturated adsorption amount and expressed as mg g^{-1}, while bT has a unit of J mol^{-1} and represents the adsorption heat parameter. The 3-parameter Temkin model has issue of having a too large 95% confidence interval, and is probably due to the parameters being intertwined [41] and having a dependency near to unity [54,77].

Jovanovic isotherm

An adsorption surface presupposition is taken into account by the Jovanovic isotherm, which is quite comparable to the Langmuir isotherm's. This scenario relates to a second estimate for localized monolayer adsorption when there are no lateral interactions present. The surface binding vibrations of an adsorbed species are taken into consideration in this model, which is the primary distinction between it and the Langmuir model [36] (**Table 3**). The isotherm also takes into account the surface binding vibrations of the adsorbed species. The Jovanovic isotherm, which encompasses three parameters, is an alternative model that takes into account the phenomenon of multilayer adsorption [36].

Table 3. Isothermal models' constants.

Model		Unit	Value	(95% confidence interval)
Freundlich#	K_F	(mg g^{-1}.L mg^{-1})$^{1/nF}$	0.62	0.548 to 0.692
	n_F	(L mg^{-1})	2.468	2.270 to 2.667
	q_{mF}	mg g^{-1}	3.39	
Temkin*‡	qmT	mg g^{-1}	0.848	Too large
	K_T	L mg^{-1}	1.287	-1.624 to 4.197
	b_T	J mol^{-1}	3.011	Too large
Langmuir	q_{mL}	mg g^{-1}	3.998	2.473 to 5.523
	b_L	L mg^{-1}	0.067	0.001 to 0.134
Jovanovic	q_{mJ}	mg g^{-1}	3.307	2.152 to 4.462
	K_J	dimensionless	0.061	0.008 to 0.114

Note
*Isotherm with *ln* term should not be plotted using data that starts from the origin (0,0)
‡Isotherms having an RT term should be plotted using the temperature (Kelvin) studied
#Isotherms that have no direct way in estimating the maximum adsorption capacity (mg g^{-1})

The removal of metals and dyes from wastewater is possible through the use of a wide variety of sorbents that have been created through coating, chemical synthesis, and various other processes [46–51]. The process of grinding of rice results in the production of a waste product known as rice husk. It is one of the most important agricultural byproducts in terms of the total volume that it produces [78,79]. According to estimates, developing nations would generate 500 million tons of rice annually, with an additional 100 million tons of rice husk that may be used. In the past, rice husks were historically utilized by the rice industry to produce blocks that are used as panels in civil construction, in addition to serving as an energy source for boilers [79,80]. However, there are a great deal more rice husks than are needed for local uses, which creates disposal issues. This material was chosen because it does not need regeneration, has a granular structure, is chemically stable, and can be produced cheaply.

CONCLUSION

Non-linear regression has been used to fit several models with one to three parameters to the data on the adsorption isotherms of Hg (II) dye onto rice husk ash. Multiple tests using a variety of metrics—including root-mean-square error (RMSE), adjusted coefficient of determination (adjR2), bias factor (BF), accuracy factor (AF), bias information coefficient (BIC), and corrected Akaike Information Criterion (AICc)—all pointed to the Freundlich model as the best option. Since the Freundlich model is based on empirical data, it cannot predict the maximum adsorption capacity. Maximum absorption was estimated to be 3.39 mg g^{-1} using the Halsey reorganization of the Freundlich equation, which is extremely comparable to the experimental measurement. Parameter values in the 95% confidence interval region are shown in the nonlinear regression method, facilitating comparison with previous research.

REFERENCE

1. Alam L, Mokhtar M, Ta GC, Lee KE, Latif MT. Environmental scan and framework of watershed risk assessment in Malaysia. In: Environmental Risk Analysis for Asian-Oriented, Risk-Based Watershed Management: Japan and Malaysia [Internet]. 2018. p. 105–21. Available from: https://www.scopus.com/inward/record.uri?eid=2-s2.0-85075846578&doi=10.1007%2f978-981-10-8090-6_8&partnerID=40&md5=38c94ec4a4006b374dc582aa9e32ced1
2. Alissa EM, Ferns GA. Heavy metal poisoning and cardiovascular disease. J Toxicol. 2011;2011:870125.
3. Sulaiman MR. Update of mercury in fish with a focus on its current status in Malaysia. J Environ Bioremediation Toxicol. 2013 Dec 27;1(1):14–9.
4. Balassone G, Aiello G, Barra D, Cappelletti P, De Bonis A, Donadio C, et al. Effects of anthropogenic activities in a Mediterranean coastland: the case study of the Falerno-Domitio littoral in Campania, Tyrrhenian Sea (southern Italy). Mar Pollut Bull. 2016;112(1–2):271–90.
5. Basri, Sakakibara M, Sera K, Kurniawan IA. Mercury contamination of cattle in artisanal and small-scale gold mining in Bombana, Southeast Sulawesi, Indonesia. Geosciences. 2017 Dec;7(4):133.
6. Goutam Mukherjee A, Ramesh Wanjari U, Renu K, Vellingiri B, Valsala Gopalakrishnan A. Heavy metal and metalloid - induced reproductive toxicity. Environ Toxicol Pharmacol. 2022 May 1;92:103859.
7. Zhao M, Li Y, Wang Z. Mercury and Mercury-Containing Preparations: History of Use, Clinical Applications, Pharmacology, Toxicology, and Pharmacokinetics in Traditional Chinese Medicine. Front Pharmacol [Internet]. 2022 [cited 2023 Aug 21];13. Available from: https://www.frontiersin.org/articles/10.3389/fphar.2022.807807
8. Crocetto F, Risolo R, Colapietro R, Bellavita R, Barone B, Ballini A, et al. Heavy Metal Pollution and Male Fertility: An Overview on Adverse Biological Effects and Socio-Economic Implications. Endocr Metab Immune Disord - Drug Targets. 2023;23(2):129–46.
9. Perrault JR, Buchweitz JP, Lehner AF. Essential, trace and toxic element concentrations in the liver of the world's largest bony fish, the ocean sunfish (Mola mola). Mar Pollut Bull. 2014;79(1–2):348–53.
10. Shi JZ, Kang F, Wu Q, Lu YF, Liu J, Kang YJ. Nephrotoxicity of mercuric chloride, methylmercury and cinnabar-containing Zhu-Sha-An-Shen-Wan in rats. Toxicol Lett. 2011;200(3):194–200.
11. Frasco MF, Fournier D, Carvalho F, Guilhermino L. Does mercury interact with the inhibitory effect of dichlorvos on *Palaemon serratus* (Crustacea: Decapoda) cholinesterase? Sci Total Environ. 2008;404(1):88–93.
12. Underwood EJ. Environmental sources of heavy metals and their toxicity to man and animals. Prog Water Technol. 1979;11(4–5):33–45.
13. Foroutan R, Peighambardoust SJ, Ahmadi A, Akbari A, Farjadfard S, Ramavandi B. Adsorption mercury, cobalt, and nickel with a reclaimable and magnetic composite of hydroxyapatite/Fe3O4/polydopamine. J Environ Chem Eng. 2021;9(4).
14. Zhang Z, Xia K, Pan Z, Yang C, Wang X, Zhang G, et al. Removal of mercury by magnetic nanomaterial with bifunctional groups and core-shell structure: Synthesis, characterization and optimization of adsorption parameters. Appl Surf Sci. 2020;500.
15. Bessa A, Gonçalves G, Henriques B, Domingues EM, Pereira E, Marques PAAP. Green Graphene–Chitosan Sorbent Materials for Mercury Water Remediation. Nanomaterials. 2020 Aug;10(8):1474.
16. Ghasemi SS, Hadavifar M, Maleki B, Mohammadnia E. Adsorption of mercury ions from synthetic aqueous solution using polydopamine decorated SWCNTs. J Water Process Eng. 2019;32.
17. Mechirackal Balan B, Shini S, Krishnan KP, Mohan M. Mercury tolerance and biosorption in bacteria isolated from Ny-Ålesund, Svalbard, Arctic. J Basic Microbiol. 2018 Apr;58(4):286–95.
18. Gasong BT, Abrian S, Sigit Setyabudi FMC. Methylmercury Biosorption Activity by Methylmercury-resistant Lactic Acid Bacteria Isolated From West Sekotong, Indonesia. HAYATI J Biosci. 2017;24(4):182–6.
19. Arshadi M, Mousavinia F, Khalafi-Nezhad A, Firouzabadi H, Abbaspourrad A. Adsorption of mercury ions from wastewater by a hyperbranched and multi-functionalized dendrimer modified mixed-oxides nanoparticles. J Colloid Interface Sci. 2017;505:293–306.
20. Song ST, Hau YF, Saman N, Johari K, Cheu SC, Kong H, et al. Process analysis of mercury adsorption onto chemically modified rice straw in a fixed-bed adsorber. J Environ Chem Eng. 2016;4(2):1685–97.
21. Hong Y, Duan Y, Zhu C, Zhou Q, She M, Du H. Experimental study on mercury adsorption of S-impregnated coconut shell activated carbon by duct injection. Dongnan Daxue Xuebao Ziran Kexue BanJournal Southeast Univ Nat Sci Ed. 2015;45(3):521–5.
22. Bandaru NM, Reta N, Dalal H, Ellis AV, Shapter J, Voelcker NH. Enhanced adsorption of mercury ions on thiol derivatized single wall carbon nanotubes. J Hazard Mater. 2013;261:534–41.
23. Peer Mohaideen MS, Srinivasan SGN, Abdul Kader JAM. Adsorption study of mercury on charcoal. Bull Electrochem. 2000;16(3):140–3.
24. Mesfin Yeneneh A, Maitra S, Eldemerdash U. Study on biosorption of heavy metals by modified lignocellulosic waste. J Appl Sci. 2011;11(21):3555–62.
25. Yeneneh AM, Thanabalan M, Demerdash UMNE. Biosorption of heavy metals by potassium hydrogen phosphate and sodium oxalate modified lignocellulosic waste. In: 2011 National Postgraduate Conference - Energy and Sustainability: Exploring the Innovative Minds, NPC 2011. 2011.
26. Younis ShA, El-Gendy NSh, El-Azab WI, Moustafa YM, Hashem AI. The biosorption of phenol from petroleum refinery wastewater using spent waste biomass. Energy Sources Part Recovery Util Environ Eff. 2014;36(23):2566–78.
27. Garg R, Garg R, Thakur A, Arif SM. Water remediation using biosorbent obtained from agricultural and fruit waste. Mater Today Proc. 2020;46:6669–72.

28. Jagaba AH, Kutty SRM, Khaw SG, Lai CL, Isa MH, Baloo L, et al. Derived hybrid biosorbent for zinc(II) removal from aqueous solution by continuous-flow activated sludge system. J Water Process Eng. 2020 Apr 1;34:101152.
29. Ag ES, Na B, Se G. Adsorption of Heavy Metal Ions from Aqueous Solutions onto Rice Husk Ash Low Cost Adsorbent. Environ Anal Toxicol. 2018;8(1):1–5.
30. Dan-Iya BI, Shukor MY. Isothermal Modelling of the Adsorption of Chromium onto Calcium Alginate Nanoparticles. J Environ Microbiol Toxicol. 2021;9(2):1–7.
31. Khare KS, Phelan FR. Quantitative Comparison of Atomistic Simulations with Experiment for a Cross-Linked Epoxy: A Specific Volume-Cooling Rate Analysis. Macromolecules. 2018;51(2):564–75.
32. Halmi MIE, Ku Ahamad KE, Shukor MY, Wasoh MH, Abdul Rachman AR, Sabullah MK, et al. Mathematical modelling of the degradation kinetics of Bacillus cereus grown on phenol. J Environ Bioremediation Toxicol. 2014;2(1):1–8.
33. Langmuir I. THE ADSORPTION OF GASES ON PLANE SURFACES OF GLASS, MICA AND PLATINUM. J Am Chem Soc. 1918;40(2):1361–402.
34. Schirmer W. Physical Chemistry of Surfaces. Z Für Phys Chem. 1999;210(1):134–5.
35. Ridha FN, Webley PA. Anomalous Henry's law behavior of nitrogen and carbon dioxide adsorption on alkali-exchanged chabazite zeolites. Sep Purif Technol. 2009;67(3):336–43.
36. Jovanović DS. Physical adsorption of gases - I: Isotherms for monolayer and multilayer adsorption. Kolloid-Z Amp Z Für Polym. 1969;235(1):1203–13.
37. Carmo AM, Hundal LS, Thompson ML. Sorption of hydrophobic organic compounds by soil materials: Application of unit equivalent Freundlich coefficients. Environ Sci Technol. 2000;34(20):4363–9.
38. Radushkevich LV. Potential theory of sorption and structure of carbons. Zhurnal Fiz Khimii. 1949;23:1410–20.
39. Dubinin MM. Modern state of the theory of volume filling of micropore adsorbents during adsorption of gases and steams on carbon adsorbents. Zh Fiz Khim. 1965;39(6):1305–17.
40. Temkin MI, Pyzhev V. Kinetics of ammonia synthesis on promoted iron catalysts. Acta Physicochim USSR. 1940;12(3):327–56.
41. Chu KH. Revisiting the Temkin Isotherm: Dimensional Inconsistency and Approximate Forms. Ind Eng Chem Res [Internet]. 2021 Aug 16 [cited 2022 Sep 1]; Available from: https://pubs.acs.org/doi/pdf/10.1021/acs.iecr.1c01788
42. Redlich O, Peterson DL. A Useful Adsorption Isotherm. Shell Dev Co Emeryv Calif. 1958;63:1024.
43. Sips R. On the structure of a catalyst surface. J Chem Phys. 1948;16(5):490–5.
44. Tóth J. Uniform interpretation of gas/solid adsorption. Adv Colloid Interface Sci. 1995;55(C):1–239.
45. Hill AV. The possible effects of the aggregation of the molecules of haemoglobin on its dissociation curves. J Physiol. 1910;40:iv–vii.
46. Khan AA, Singh RP. Adsorption thermodynamics of carbofuran on Sn (IV) arsenosilicate in H+, Na+ and Ca2+ forms. Colloids Surf. 1987;24(1):33–42.
47. Brunauer S, Emmett PH, Teller E. Adsorption of Gases in Multimolecular Layers. J Am Chem Soc. 1938;60(2):309–19.
48. Vieth WR, Sladek KJ. A model for diffusion in a glassy polymer. J Colloid Sci. 1965;20(9):1014–33.
49. Radke CJ, Prausnitz JM. Adsorption of Organic Solutes from Dilute Aqueous Solution of Activated Carbon. J Am Chem Soc. 1972;11(4):445–51.
50. Hamissa AMB, Brouers F, Mahjoub B, Seffen M. Adsorption of Textile Dyes Using Agave Americana (L.) Fibres: Equilibrium and Kinetics Modelling. Adsorpt Sci Technol. 2007 Jun 1;25(5):311–25.
51. Fritz W, Schluender EU. Simultaneous adsorption equilibria of organic solutes in dilute aqueous solutions on activated carbon. Chem Eng Sci. 1974;29(5):1279–82.
52. Chu KH, Tan B. Is the Frumkin (Fowler–Guggenheim) adsorption isotherm a two- or three-parameter equation? Colloid Interface Sci Commun. 2021 Nov 1;45:100519.
53. Martucci A, Braschi I, Bisio C, Sarti E, Rodeghero E, Bagatin R, et al. Influence of water on the retention of methyl tertiary-butyl ether by high silica ZSM-5 and Y zeolites: A multidisciplinary study on the adsorption from liquid and gas phase. RSC Adv. 2015;5(106):86997–7006.
54. Motulsky HJ, Ransnas LA. Fitting curves to data using nonlinear regression: a practical and nonmathematical review. FASEB J. 1987;1(5):365–74.
55. Burnham KP, Anderson DR. Multimodel inference: Understanding AIC and BIC in model selection. Sociol Methods Res. 2004;33(2):261–304.
56. Akaike H. A New Look at the Statistical Model Identification. IEEE Trans Autom Control. 1974;19(6):716–23.
57. Homagai PL, Poudel R, Poudel S, Bhattarai A. Adsorption and removal of crystal violet dye from aqueous solution by modified rice husk. Heliyon. 2022;8(4):e09261.
58. Langmuir I. The constitution and fundamental properties of solids and liquids. Part I. Solids. J Am Chem Soc. 1916;38(11):2221–95.
59. Foo KY, Hameed BH. Insights into the modeling of adsorption isotherm systems. Chem Eng J. 2010;156(1):2–10.
60. Freundlich H. Über die adsorption in lösungen (Over the adsorption in solution). Z Für Phys Chem. 1907;57(1):385–470.
61. Barkhordar B, Ghias Aldin M. Comparision of Langmuir and Freundlich equilibriums in Cr, Cu and Ni adsorption by Sargassum. Iran J Environ Health Sci Eng. 2004 Jan 1;1(2):58–64.
62. Crittenden JC, Watson HM. Adsorption. In: MWH's Water Treatment: Principles and Design, Third Edition [Internet]. John Wiley & Sons, Ltd; 2012 [cited 2020 May 31]. p. 1117–262. Available from: https://onlinelibrary.wiley.com/doi/abs/10.1002/9781118131473.ch15
63. Al-Ghouti MA, Da'ana DA. Guidelines for the use and interpretation of adsorption isotherm models: A review. J Hazard Mater. 2020 Jul 5;393:122383.
64. Hu Q, Pang S, Wang D. In-depth Insights into Mathematical Characteristics, Selection Criteria and Common Mistakes of Adsorption Kinetic Models: A Critical Review. Sep Purif Rev. 2021 Jul 1;0(0):1–19.
65. Baker H. Removal of Lead Ions from Waste Water Using Modified Jordanian Zeolite. Chem Sci Int J. 2020 Nov 9;19–30.
66. Liyanage LMM, Lakmali WGM, Athukorala SNP, Jayasundera KB. Application of live Chlorococcum aquaticum biomass for the removal of Pb(II) from aqueous solutions. J Appl Phycol. 2020 Dec 1;32(6):4069–80.
67. Ahmad R, Mirza A. Synthesis of Guar gum/bentonite a novel bionanocomposite: Isotherms, kinetics and thermodynamic studies for the removal of Pb (II) and crystal violet dye. J Mol Liq. 2018 Jan 1;249:805–14.
68. Daifullah A a. M, Moloukhia H. Removal of cobalt and europium radioisotopes using activated carbon prepared from apricot stones. Isot Radiat Res [Internet]. 2002 Jul 1 [cited 2022 Jul 26];34. Available from: https://www.osti.gov/etdeweb/biblio/20395653
69. Moloukhia H, El-Zakla T, Belacy N. Use of lignocellulosic biomass in removal of 60 Co and 13'4 Cs from radioactive wastewater. Arab J Nucl Sci Appl. 2010;43(1):121–30.
70. Rajapaksha AU, Vithanage M, Jayarathna L, Kumara CK. Natural Red Earth as a low cost material for arsenic removal: Kinetics and the effect of competing ions. Appl Geochem. 2011 Apr 1;26(4):648–54.
71. Mahapatra A, Mishra BG, Hota G. Electrospun Fe2O3–Al2O3 nanocomposite fibers as efficient adsorbent for removal of heavy metal ions from aqueous solution. J Hazard Mater. 2013 Aug 15;258–259:116–23.
72. Sharifi S, Nabizadeh R, Akbarpour B, Azari A, Ghaffari HR, Nazmara S, et al. Modeling and optimizing parameters affecting hexavalent chromium adsorption from aqueous solutions using Ti-XAD7 nanocomposite: RSM-CCD approach, kinetic, and isotherm studies. J Environ Health Sci Eng. 2019 Dec 1;17(2):873–88.
73. Calderón C, Levío-Raimán M, Diez MC. Cadmium removal for marine food application: comparative study of different adsorbents. Int J Environ Sci Technol [Internet]. 2021 Oct 29 [cited 2022 Jul 26]; Available from: https://doi.org/10.1007/s13762-021-03746-9
74. Yakubu A, Olatunji GA, Adekola FA. Modified/Unmodified Nanoparticle Adsorbents of Cellulose Origin With High Adsorptive Potential for Removal of Pb(II) From Aqueous Solution. Eur Sci J ESJ. 2017 Sep 30;13(27):425–425.

75. Rushton G, Karns C, Shimizu K. A critical examination of the use of the Freundlich isotherm in characterizing molecularly imprinted polymers (MIPs). Anal Chim Acta. 2005 Jan 3;528:107–13.
76. Hamdaoui O, Naffrechoux E. Modeling of adsorption isotherms of phenol and chlorophenols onto granular activated carbon: Part I. Two-parameter models and equations allowing determination of thermodynamic parameters. J Hazard Mater. 2007 Aug 17;147(1):381–94.
77. Knott G, Shrager R. On-line modeling by curve-fitting. SIGGRAPH Comput Graph. 1972;6(4):138–51.
78. Daifullah AAM, Girgis BS, Gad HMH. Utilization of agro-residues (rice husk) in small waste water treatment plans. Mater Lett. 2003;57(11):1723–31.
79. Abdelwahab O, Nemr A El, El-Sikaily A, Khaled A. Use of rice husk for adsorption of direct dyes from aqueous solution: A case study of direct F. Scarlet Green synthesis of TiO2 nanoparticles and its toxicity View project Industrial valorization of local biological materials and wastes for wastewater tre. Egypt J Aquat Res. 2005;31(May).
80. Della VP, Kühn I, Hotza D. Caracterização de cinza de casca de arroz para uso como matéria-prima na fabricação de refratários de sílica. Quimica Nova. 2001;24(6):778–82.